TECHNICAL REPORT 28

MEASUREMENT OF CESIUM EXCITATION CROSS SECTION NEAR THRESHOLD BY A SWARM TECHNIQUE

J. F. NOLAN AND A. V. PHELPS

ARPA Order Number: 125-63 (Amd. 11)

Contract Number: NONR-2584(00)

Project Code: 4720

Atomic & Molecular Sciences
Research & Development
Westinghouse Research Laboratories
Pittsburgh, Pennsylvania 15235

April 15, 1965

This research is a part of Project DEFENDER, sponsored by the Advanced Research Projects Agency, Department of Defense.

TECHNICAL REPORT 28

MEASUREMENT OF CESIUM EXCITATION CROSS SECTION NEAR THRESHOLD BY A SWARM TECHNIQUE

J. F. NOLAN AND A. V. PHELPS

ARPA Order Number: 125-63 (Amd. 11)

Contract Number: NONR-2584(00)

Project Code: 4720

Atomic & Molecular Sciences
Research & Development
Westinghouse Research Laboratories
Pittsburgh, Pennsylvania 15235

April 15, 1965

This research is a part of Project DEFENDER, sponsored by the Advanced Research Projects Agency, Department of Defense

MEASUREMENT OF CESIUM EXCITATION CROSS SECTION NEAR THRESHOLD BY A SWARM TECHNIQUE*

J. F. Nolan and A. V. Phelps
Westinghouse Research Laboratories, Pittsburgh, Pennsylvania

ABSTRACT

Electron drift velocities have been measured in cesium-argon mixtures for E/N values between 3×10^{-19} and 5×10^{-18} V-cm^2 and cesium to argon concentration ratios between 10^{-8} and 10^{-5}. The drift velocity was obtained from measurements of the electron transit time using an ac technique which is a modification of a technique developed originally by Rutherford for ion drift velocity measurements. Numerical solutions of the Boltzmann transport equation were used to determine an excitation cross section which is consistent with the experimental drift velocity data. For a single excitation threshold at 1.386 eV, the best slope for a linear cross section is 7.1×10^{-15} cm^2/eV. If excitation to the 6 $P_{1/2}$ and 6 $P_{3/2}$ states is considered separately, with thresholds at 1.386 eV and 1.454 eV respectively, the linear cross sections obtained have a slope of 2.5×10^{-15} cm^2/eV for 6 $P_{1/2}$ excitation, and 5.0×10^{-15} cm^2/eV for 6 $P_{3/2}$ excitation. The range of validity of these values is from threshold up to about 1.8 eV. Other shapes for the cross section are investigated. The experimental cross section is in reasonable agreement with extrapolations of theoretical cross sections.

---

* This work was supported in part by the Advanced Research Projects Agency through the Office of U.S. Naval Research.

I. INTRODUCTION

Collisions between electrons and cesium atoms have been the subject of numerous experimental investigations. Measurements have been reported for the total,[1] momentum transfer,[2-9] and ionization[10,11] cross sections. Experimental information on relative excitation cross sections for cesium has become available only quite recently, when Bogdanova[12] and Zapesochnyi and Shimon[13] reported measurements of excitation functions for some of the spectral lines of cesium. These experiments give the shape of the excitation function for several cesium lines, including one of the resonance lines. The present paper presents the results of a measurement of the cesium excitation cross section as obtained from analysis of electron drift velocity measurements. The measurements are made in a mixture of cesium and argon, rather than in pure cesium vapor since the presence of the Ramsauer minimum in argon serves to amplify the effect of low energy electrons produced by inelastic collisions. The drift velocity is measured as a function of E/N, the ratio of electric field to total gas density, and also as a function of N_{Cs}/N_{Ar}, the ratio of cesium to argon density. The method used to measure the drift velocity is a modification of an ac technique developed originally by Rutherford[14] for the measurement of ion drift velocities and used by Loeb[15] and Wahlin[16] for electrons. The data is analyzed to give the cross section for electron excitation of cesium in the energy range from threshold to a few tenths of an eV above threshold. The analysis of the data makes use of a numerical solution of the Boltzmann equation to give the appropriate

electron energy distribution function; i.e., no a priori assumptions are made about the shape of the distribution function. It is found that a linear cross section gives a good fit to the data in the range covered. Other shapes for the cross section are considered. The experimental cross section is compared with several theoretical calculations.

II. METHOD

The essential features of the method used to measure the drift velocity are illustrated schematically in Fig. 1. The electrode structure is a parallel plate condenser with a guard ring around one of the plates to provide uniformity of the electric field in the central region. To understand the operation of the tube, suppose that there is a steady source of electrons at the plate shown on the left (the cathode) and a voltage square wave is applied to this electrode. The right hand electrode (the anode) is at a potential which is essentially ground potential, i.e., it is within a few millivolts of ground. For the positive half-cycle of the square wave, the field is in a direction such that electrons do not drift across the tube. For the negative half-cycle, the electrons drift from the cathode toward the anode, and two cases can be distinguished. First, suppose that the half-period, T, of the square wave is less than τ, the electron drift time across the gap. In this case the direction of the field reverses before the electrons reach the anode, and in the positive half cycle they drift back toward the cathode. It is clear that if we have a dc meter in the anode circuit, the induced currents cancel out and the average current, I, is zero.

If T is greater than τ, the field acts in the right direction long enough to allow some electrons to reach the anode, and there will be a non-zero dc anode current. If the current available from the cathode is i_o, the magnitude of the average current collected at the anode is the charge collected during the time $T - \tau$ divided by the period of the square wave $2T$, i.e.,

$$I = \frac{i_o(T - \tau)}{2T} = \frac{i_o}{2}(1 - \tau/T). \tag{1}$$

In terms of the frequency, f, of the applied square wave, we have

$$I = \frac{i_o}{2}(1 - 2\tau f) \quad \text{for} \quad f < \frac{1}{2\tau}, \tag{2}$$

and

$$I = 0 \quad \text{for} \quad f > \frac{1}{2\tau}. \tag{3}$$

It is seen that if the average current is plotted as a function of the frequency, a curve is obtained (solid curve in Fig. 2) which decreases linearly up to the point where $T = \tau$ and is zero thereafter. In terms of frequency, the break in the curve occurs at a frequency given by $f = \frac{1}{2\tau}$. By this means it is possible to measure the electron drift time, τ, by observing the break point in the current versus frequency curves. Knowing the drift distance then enables one to obtain the drift velocity.

The description just given is a simplification of the actual experimental situation in two respects. First, we have neglected diffusion. The main effect of diffusion is to round off the sharp break indicated by the solid curve in Fig. 2, since some electrons drift across in time less than τ and others in time greater than τ. Secondly, in the actual experimental situation, both electrodes act as sources of electrons. The electrons are obtained by thermionic emission from the two electrodes at the equilibrium temperature of the tube, which is about 250°C. The thermionic emission from the two electrodes is comparable but not equal, since there is a difference of a few degrees in temperature between them caused by a better heat sink to the outside from one of them. If the thermionic currents available from the two electrodes are designated as i_1 and i_2, and if the amplitude of the positive half-cycle of the applied square wave is equal in magnitude to that of the negative half-cycle then the effect of emission from both electrodes is to replace i_o by $i_1 - i_2$ in Eqs. (2) and (3).

Figure 2 shows a typical curve for the average anode current vs. frequency of the square wave. The break point is obtained by extending the linear regions at high and low frequencies until they intersect. In order to reduce end effects, the drift time was measured as a function of the drift distance, with E/N held constant, and the drift velocity was taken from the slope of τ vs d curves. The τ vs d curves were linear but did not, in general, go through the origin Figure 3 shows a typical example. The extrapolated value of τ at d = 0 was never more than 10% of the value of τ at the largest value of d.

III. APPARATUS

A schematic diagram of the vacuum system is shown in Fig. 4. The drift tube is contained in an oven which in these experiments operated in the range 250-300°C. The cesium was contained in a U-tube in a separate oven whose temperature could be controlled independently of the main oven. The vapor pressure of the cesium in the drift tube was controlled by controlling the temperature of the cesium reservoir.

The drift region consists of two parallel plate electrodes made of advance (nickel-copper alloy) as shown in Fig. 1. The position of one of the electrodes could be varied through a bellows arrangement in the vacuum wall. This allowed for a range of spacings between the two electrodes from 0.05 cm to 1 cm. A cathetometer was used to measure the distance between the electrodes with the drift tube enclosed in a glass envelope and evacuated to the operating pressures. The distance was measured as a function of the reading of the micrometer dial on the driver assembly which was used to vary the spacing. During the drift velocity measurements the tube was encased in a stainless steel envelope, so that the distance was obtained from the calibration chart.

The circuitry used in the measurements is shown in block diagram form in Fig. 1. A sine wave generator produced a sine wave of twice the frequency desired for the square wave applied to the tube. This was then converted into a square wave at half frequency. This conversion from 2 f to f was required in order to maintain good symmetry of the square wave

over the entire frequency range. The square wave then went through two stages of amplification and was fed through a cathode follower into the cathode of the drift tube. To minimize the ac signal on the anode of the tube due to coupling of the cathode wave form across the tube, a portion of the cathode wave form is inverted and fed through a variable impedance (designated ac bridge in Fig. 1) to the anode. This adjustment was not critical; i.e., the coupling was always small. The average anode current was measured by several techniques. The method used for most of the measurements presented here was to measure the voltage developed across a 10^4 Ω load resistor with a micro-voltmeter. This constituted the dc ammeter shown in Fig. 1. The leakage resistance from the anode to ground was usually 10^6 to 10^7 ohms, so that a high impedance ammeter could not be used. The average current at the anode was in the range 10^{-10} to 10^{-8} amperes.

The rise time of the square wave (to 90% of full amplitude) was about 15 nanoseconds. The voltage of the negative half of the square wave was set by applying a dc potential (negative with respect to ground) to the cathode circuit of the cathode follower in series with the cathode resistor. During the negative portion of the square wave the cathode follower tube does not conduct, so that the bottom of the square wave is set at the potential of the dc source, which is monitored by a dc voltmeter. The square wave applied to the drift tube is taken from a variable portion of the cathode resistor. The amplitude could be varied between zero and 50 volts. An additional dc voltemeter monitored the average voltage of the square wave

with respect to its lowest voltage. With the negative portion of the square wave set at - V volts, a reading of V on this meter insures that the square wave has total amplitude 2V, with equal positive and negative amplitudes with respect to ground. A condition on the preceding statement is that the square wave should have good time symmetry and be free from any significant distortion. This was checked by observing the wave form on a cathode ray oscilloscope. The square wave was time symmetric to within 3% for all frequencies. The field E was computed from the relation $E = V/d$ where V is half the total square wave voltage and d is the distance between electrodes.

IV. PRESSURE MEASUREMENTS

In evaluating the data it was necessary to know the cesium density, N_{Cs}, and the argon density, N_{Ar}. The argon density was obtained from the total pressure as measured by the null indicating manometer. In all cases the cesium pressure was much less than the argon pressure (ratio 10^{-5} or less) so that the total pressure was equal to the argon pressure to a very good approximation. The cesium vapor pressure was calculated from the expression found by Taylor and Langmuir[17]

$$\log_{10} P = 11.0531 - \frac{4041}{T} - 1.35 \log_{10} T \qquad (4)$$

where P is the vapor pressure in mm Hg and T is the temperature of the cesium reservoir in ^{o}K. It is believed that this expression gives an accurate representation of the equilibrium cesium vapor pressure as a function of

temperature; recent measurements by Marino, et al[18] are in very good agreement with Eq. (4). The main problem in the present measurements was to make sure that equilibrium had been reached, so that Eq. (4) could be used to calculate the cesium pressure.

The procedure followed in obtaining a cesium-argon mixture was to set the cesium reservoir temperature to give the desired cesium pressure, then admit argon to the desired pressure and close the by-pass valve (Fig. 4). It was initially expected that the time required for equilibrium to be reached would be of the order of an hour. However, drift velocity measurements revealed that, at a given value of E/N, the drift velocity changed slowly by about 20% of its departure from the value for pure Ar over a period of several days and did not become constant with time until about three days after the mixture was prepared.[19] The measurements presented here are the long time measurements when the drift velocity was constant with time; the cesium pressure is assumed to have reached its equilibrium value and is computed from Eq. (4). The long time required to reach equilibrium has been found by others working with cesium,[20] and is presumed to be due to a combination of diffusion and wall-coating effects.

One possible alternative explanation for this change with time is to assume that the cesium reacts chemically with some impurity coming off the walls of the vacuum system, so that cesium atoms are, in effect, removed from the system at a constant rate. If this were the case, it would be possible to arrive at a steady state cesium density which is determined not by the

reservoir temperature but by the rate of reaction. To check this possibility, the drift velocity was remeasured with the drift tube at a higher temperature, such that the rate at which impurities were given off by the vacuum walls was increased by a factor of four. This factor of four increase in impurity buildup was known from previous measurements of the rate of rise of pressure in the vacuum system as a function of temperature, before the cesium ampule was broken. The result of this test was that the measured drift velocity agreed with the previously determined value. This increases our confidence that the cesium pressure in the drift region does in fact correspond to the equilibrium vapor pressure at the reservoir temperature.

V. RESULTS

The drift velocity was measured as a function of E/N for several values of N_{Cs}/N_{Ar}. For $N_{Cs}/N_{Ar} < 10^{-7}$ the cesium had no effect on the drift velocity; i.e., the drift velocity measured was characteristic of pure argon. The present results for low density ratios are compared with the results of Pack and Phelps[21] as shown by the lower curve of Fig. 5. The square data points are those obtained in the present work for density ratios less than 10^{-7}. The agreement is good, and this serves as a useful check on the present method of measuring drift velocities.

For larger values of N_{Cs}/N_{Ar}, the drift velocity departs from the pure argon value in the E/N range above 5×10^{-19} V-cm^2. The circular data points in Fig. 5 show the value of drift velocity obtained for a constant density ratio of $\frac{N_{Cs}}{N_{Ar}} = 6.9 \times 10^{-6}$.

A qualitative explanation for the change in drift velocity due to the presence of the cesium is as follows: In the E/N region above 5×10^{-19} V-cm^2, the electrons in the high energy tail of the distribution are energetic enough to excite cesium atoms to the first excited state. The threshold energy is 1.386 eV.[22] When such a collision occurs, the electron is left with very little energy. That is, it is transferred from the high energy tail of the distribution function to the low energy region, where the cross section for electron-argon collisions is much lower due to the Ramsauer minimum. This lower effective cross section results in a higher drift velocity, so that the effect of inelastic collisions with cesium atoms is to increase the drift velocity above that in pure argon.

The momentum transfer cross section for electron-argon collisions is known,[23] so that the present data may be used to obtain the cross section for excitation of cesium by electrons. The method of analysis of the data is discussed in the next section.

VI. ANALYSIS OF DATA

In order to obtain the cross section as a function of electron energy from the drift velocity as a function of E/N, it is necessary to know the electron energy distribution function. In general, however, one does not know the shape of the distribution function a priori. The assumption of a Maxwellian or Druyvesteynian shape is not justified under the conditions

of the present experiments. The procedure followed is to assume an excitation cross section with the proper threshold as a function of electron energy and to use this cross section in obtaining a numerical solution of the Boltzmann equation. This gives the distribution function appropriate to the assumed cross section, so that the drift velocity can then be calculated as a function of E/N. This "theoretical" drift velocity is then compared to the experimental values, and the input cross section is adjusted in magnitude and shape until the two drift velocities agree. This allows one to obtain a cross section which is consistent with the experimental results. The final cross section obtained in this way is not unique in that rapid changes with energy in the cross section curve will be at least partially averaged out because of the relatively large spread in the electron energy distribution.

The analysis of the drift velocity data in the present work is similar to that used by Frost and Phelps[24] and by Engelhardt and Phelps,[25] and will not be presented in any detail here. The basis of the analysis is Eq. (2) of reference 25.

Since N_{Cs} is always less than 10^{-5} N_{Ar}, the contribution of Cs to the effective momentum transfer scattering cross section for the mixture is negligible for all cases considered in this paper. The momentum transfer cross section used for Ar is that given by Frost and Phelps.[23] A discussion of available momentum transfer cross section data for Cs is given in Appendix I of this paper. The negligible contribution of Cs to the momentum transfer cross section is borne out experimentally by the fact that for

E/N low enough that inelastic collisions cannot occur to any appreciable extent, the drift velocity agrees with the drift velocity in pure argon.

In the present case we are concerned only with the excitation of cesium since the excitation of the electronic states of Ar is negligible at the E/N considered. Since all of the parameters which enter into Eq. (2) of reference 25 are known, with the exception of the excitation cross section for Cs, Q_j, it is possible to obtain by numerical methods a curve of Q_j vs. energy which is consistent with the experimental measurements and with the known cross section in argon. This was done for several different shapes for Q_j. The solid curves in Fig. 5 labeled "linear," "optical," and "classical" are the drift velocities calculated using three different shapes for the excitation cross section. The linear cross section is simply a straight line starting at threshold and continuing upward indefinitely. The "optical" cross section has a shape based on the experimentally observed shape for the excitation function for cesium resonance radiation.[13] The "classical" cross section has a shape given by the equation

$$Q_j(\epsilon) = \frac{Q_o\ (\epsilon - \epsilon_o)}{\epsilon^2} \qquad (5)$$

where ϵ is the electron energy and ϵ_o is the threshold energy.[26]

It will be seen from Fig. 5 that agreement with experiment can be obtained for all three of these shapes, provided appropriate magnitudes are chosen. The magnitudes required to give the agreement are shown in Fig. 6. It will be noted that all three curves are in agreement . . the

energy range from threshold up to about 1.8 eV, but diverge at higher energies. This reflects the fact that, for the experimental conditions used, there are not many electrons with energies higher than 1.8 eV, so that the experiment is most sensitive to the initial slope of the cross section. The effective initial slope of the cross section, obtained from the slope of the straight line which gives best agreement with experiment is 7.1×10^{-15} cm^2/eV.

A cross section varying as the square root of the excess energy[27] was tried, but it was found that the agreement with experiment was not as good in this case as for a linear cross section. Consequently, the results are presented in terms of an effective linear cross section near threshold, even though the detailed shape of the cross section may not in fact be linear.

Calculations were also performed assuming cross sections for excitation to the two excited 6P states: the $6P_{1/2}$ state with threshold at 1.386 eV and the $6P_{3/2}$ state with threshold at 1.454 eV.[22] Linear shapes were assumed for both cross sections and it was also assumed that the ratio of the slopes of the $6P_{3/2}$ to the $6P_{1/2}$ curves was two to one, the ratio of the statistical weights.[28] Comparison of the results of this calculation with experiment are shown in Fig. 7. The best values obtained for the slopes were 2.5×10^{-15} cm^2/eV for excitation to the $6P_{1/2}$ state and 5×10^{-15} cm^2/eV for excitation to the $6P_{3/2}$ state. The drift velocity calculated from this "two threshold" case gives a little better fit to

the experimental data in the E/N region around 10^{-18} V/cm^2, but the precision of the data is not good enough to indicate a clear preference for the two threshold case over the single threshold case.

No calculations were made including any higher excited states since states higher than the 6P states are not expected to have any significant effect on the drift velocity. The reason for this is that the cross sections for excitation to higher states are expected to be small compared to the cross section for excitation to the resonance states. At high energies, where the Born approximation is valid, the relative magnitude of the cross sections for excitation to various levels varies as the oscillator strength for the transition involved. In cesium the oscillator strengths for transitions between the resonance 6P state and the ground state are very large (a factor of 40 or more) compared to those for other states.[29] Although Born approximation predictions are not expected to be valid at the low energies involved in the present case, calculations by Seaton[30] indicate that the oscillator strength can be used as a rough guide to the magnitude of the excitation cross section at low energies. In the case of potassium there is experimental evidence that the magnitude of the excitation cross section varies roughly as the oscillator strength.[31] Consequently, only excitation to the 6P states has been considered in the analysis of the present data.

VII. DISCUSSION

The excitation cross section for cesium has been obtained in the region close to threshold in the form of the slope of an effective linear cross section. In the energy range covered it was found that the experimental data could also be analyzed in terms of cross section shapes other than linear; the results are presented in terms of a linear cross section because of its simplicity. For a single threshold cross section, the best slope is 7.1×10^{-15} cm^2/eV. For a two threshold cross section, the best slopes are 2.5×10^{-15} cm^2/eV for $6P_{1/2}$ excitation, and 5.1×10^{-15} cm^2/eV for $6P_{3/2}$ excitation. The range of validity of these values is from threshold up to about 1.8 eV. If there is no systematic error present in the measurements, the above values are accurate to about $\pm$ 20%; i.e., if the slope of the assumed cross section is changed by $\pm$ 20%, the calculated curve of drift velocity vs. E/N is clearly not a good fit to the experimental points.

Theoretical calculations of the cross section for 6S-6P excitation have been reported by Hansen,[32] Witting,[33] and by Vainshtein, et al.[34] A comparison of the present experimental results with these theoretical calculations is of limited value, since the experimental results are valid in the region just above threshold, while the theoretical calculations are most reliable at higher energies and are not expected to be accurate in the threshold region. Nevertheless such a comparison is of interest, and is given in Fig. 8. The present results are shown for two shapes,

the linear, single threshold shape, and the "optical" shape. It is seen that the "optical" cross section is in reasonable agreement with the theor tical calculations of Witting and of Hansen, and lies somewhat higher than the calculation of Vainshtein, et al. It is believed that the present results do not show a clear preference for the Witting calculations over those of Hansen, since the accuracy of our "optical" curve is limited by the accuracy with which it is possible to obtain the initial slope from the graph presented in reference 13. Witting[33] has estimated the initial slope of the cross section to be 7.5×10^{-15} cm^2/eV, which is in good agreement with the value of 7.1×10^{-15} cm^2/eV derived from the present measurements.

Tabulations of the experimental data are given in Appendix II.

ACKNOWLEDGEMENTS

The authors wish to express their appreciation for many valuable discussions with their associates in the Atomic Physics Group. In particular they wish to acknowledge the assistance rendered by J. L. Pack in the electronic instrumentation and A. G. Engelhardt in the numerical calculations. They wish also to acknowledge the assistance given by R. L. Fry and H. T. Garstka in the construction of the drift tube and associated vacuum system.

APPENDIX I

MOMENTUM TRANSFER CROSS SECTION IN CESIUM

In the analysis of the data in Sect. VI the values used for the momentum transfer cross section for cesium were taken from Brode[1] at high electron energies and from Boeckner and Mohler as corrected by one of us (AVP) at low electron energies. It is the purpose of this appendix to outline the steps involved in making the correction and to apply an additional correction to the data of Boeckner and Mohler.

The cross section as originally found by Boeckner and Mohler is shown in column 2 of Table I. The reduced collision frequency, ν/N, calculated from the uncorrected data is shown in column 3, where the reduced collision frequency is given by

$$\frac{\nu}{N} = \frac{e}{m} \frac{1}{\mu N} \tag{6}$$

where ν is the collision frequency, N is the gas density, e and m are the charge and mass of the electron, and μ is the electron mobility as given in Eq. (2) of reference 2. Boeckner and Mohler obtained the cesium cross sections by plotting the total observed cross section versus cesium ion density and extrapolating to zero ion or electron density to get the cross section for cesium atoms. In a later paper[35] it was found from spectroscopic measurements that the electron densities obtained with the Langmuir probe were in error for cesium pressures above 3×10^{-3} mm Hg. If one applies

this electron density correction one obtains the values of ν/N shown in column 4 of Table 1. These values are essentially independent of electron energy and were the basis for the result cited by Frost.[36]

It is to be noted that the collision frequency obtained from Eq. (6) is an effective collision frequency, averaged over a Maxwellian distribution of electron energies. However, since the effective collision frequency is found to be independent of energy for the range covered, one can conclude that the experimental results are consistent with a monoenergetic collision frequency which is constant with energy. The monoenergetic momentum transfer cross section is then given by

$$Q_m = \left(\frac{\nu}{N}\right) \quad v^{-1} \tag{7}$$

where v is the electron velocity.

It now appears that the relation used by Boeckner and Mohler to calculate the cesium pressure is in error. If one uses Eq. (4) to correct the pressures given by Boeckner and Mohler, one obtains the reduced collision frequency given in column 5 of Table 1. It is seen that the reduced collision frequency has a smaller magnitude and is fairly constant with energy. It is believed that a reasonable value to take from the work of Boeckner and Mohler is a constant reduced collision frequency of 1.1×10^{-6} $cm^3/sec.$; this is used to calculate the momentum transfer cross section shown in Fig. 9, labeled Boeckner and Mohler (revised).[37]

Also shown in Fig. 9 are a number of other experimental measurements of the momentum transfer cross section in cesium. The Brode curve in Fig. 9 represents the total cross section as obtained from measurements with a monoenergetic electron beam; all of the other curves shown are obtained from experiments which involve a distribution of electron energies. Ideally, one would like to derive monoenergetic cross sections from these experiments so that the comparison will be more meaningful. This has been done for some, but not all, of the curves shown in Fig. 9. Chen and Raether[5] give an expression for the monoenergetic Q_m; this expression was used to plot their results. Meyerand and Flavin[9] have also taken the energy dependence of the cross section into account. Roehling[8] gives values for the averaged cross section at various temperatures; his data are represented in Fig. 9 by a smooth curve drawn through these values with the electron energy taken to be kT. The data of Harris[7] and Mullaney and Dibelius[4] are plotted assuming that the collision frequency they measured was constant from $\frac{1}{2}$ kT to 2 kT. Morgulis and Korchevoi[6] give a value of 5×10^{-15} cm^2 for the momentum transfer cross section at an electron temperature of $\sim$ $5000^{\circ}K$; this value is plotted with the electron energy taken to be kT. The data of Steinberg[3] is not plotted in Fig. 9, since it is believed that these measurements were subject to errors similar to those discussed above in the case of Boeckner and Mohler, but of unknown magnitude.

It will be seen from Fig. 9 that there is still considerable uncertainty in the low energy momentum transfer cross section, but that the cross section is low enough not to be important in the analysis of Sect. VI.

REFERENCES

1. R. B. Brode, Phys. Rev. 34, 673 (1929).
2. C. Boeckner and F. L. Mohler, Bur. Std. J. Res. 10, 357 (1933).
3. R. K. Steinberg, J. Appl. Phys. 21, 1028 (1950).
4. G. J. Mullaney and N. R. Dibelius, A.R.S. Journal 31, 1575 (1961).
5. C. L. Chen and M. Raether, Phys. Rev. 128, 2679 (1962).
6. N. D. Morgulis and Y. P. Korchevoi, Soviet Phys.-Tech. Phys. 7, 655 (1963).
7. L. P. Harris, J. Appl. Phys. 34, 2958 (1963).
8. D. Roehling, Adv. Energy Conv. 3, 69 (1963).
9. R. G. Meyerand and R. K. Flavin, Atomic Collision Processes, edited by M.R.C. McDowell, North Holland Publ. Co., Amsterdam (1964), p. 59.
10. J. T. Tate and P. T. Smith, Phys. Rev. 46, 773 (1934).
11. G. O. Brink, Phys. Rev. 134, A345 (1964).
12. I. P. Bogdanova, Bull. Acad. Sci. USSR, Phys. Ser. 24, 958 (1960).
13. I. P. Zapesochnyi and L. L. Shimon, Opt. Spectry (USSR) 16, 504 (1964).
14. E. Rutherford, Phil. Mag. 44, 422 (1897).
15. L. B. Loeb, Phys. Rev. 19, 24 (1922); 20, 397 (1922); and 23, 157 (1924).
16. H. B. Wahlin, Phys. Rev. 21, 517 (1923); 23, 169 (1924); 27, 588 (1926); and 37, 260 (1931).
17. J. B. Taylor and I. Langmuir, Phys. Rev. 51, 753 (1937).
18. L. L. Marino, A.C.H. Smith, and E. Caplinger, Phys. Rev. 128, 2243 (1962).

19. In a preliminary report of these measurements, drift velocities measured after a few hours were used to obtain a cross section some 30% higher than that presented here. See J. F. Nolan and A. V. Phelps, Bull. Am. Phys. Soc. 8, 445 (1963).

20. J. R. Fendley, Jr., Report on the Thermionic Conversion Specialist Conference, October 1963, p. 129.

21. J. L. Pack and A. V. Phelps, Phys. Rev. 121, 798 (1961).

22. C. E. Moore, "Atomic Energy Levels," U.S. Dept. of Commerce, N.B.S., Vol. III, May 1, 1958, p. 124.

23. L. S. Frost and A. V. Phelps, Phys. Rev. 136, A1538 (1964).

24. L. S. Frost and A. V. Phelps, Phys. Rev. 127, 1621 (1962).

25. A. G. Engelhardt and A. V. Phelps, Phys. Rev. 131, 2115 (1963).

26. J. J. Thomson, Phil. Mag. 23, 449 (1912). See also M. J. Seaton in "Atomic and Molecular Processes," edited by D. R. Bates, Academic Press, New York, p. 395.

27. E. P. Wigner, Phys. Rev. 73, 1002 (1948). A discussion of threshold laws as applied to excitation of atoms by electrons can be found in E. Gerjuoy, J. Appl. Phys. 30, 28 (1959) and E. Gerjuoy, Rev. Mod. Phys. 33, 544 (1961).

28. The assumption that the magnitudes of the two excitation cross sections have the ratio of the statistical weights has received experimental support in the case of potassium, where the excited levels involved are the $4P_{1/2}$ and $4P_{3/2}$ states. See L. M. Volkova and A. M. Devyatov, Bull. Acad. Sci. USSR 27, 1025 (1963).

29. P. M. Stone, Phys. Rev. 127, 1151 (1962).

30. M. J. Seaton, Proc. Phys. Soc. (London) 79, 1105 (1962).

31. L. M. Volkova, Opt. Spectry. (USSR) 6, 179 (1959); L. M. Volkova and A. M. Devyatov, Bull. Acad. Sci. USSR 27, 1025 (1963); E. M. Anderson and V. A. Zilitis, Opt. Spectry. (USSR) 16, 99 (1964).

32. L. K. Hansen, J. Appl. Phys. 35, 254 (1964).

33. H. L. Witting, Quarterly Progress Report No. 70, Research Laboratory of Electronics, MIT (July 1963), p. 153.

34. L. Vainshtein, V. Opyktin, and L. Presnyakov, Zhur Eksp. i Teoret. Fiz. 47, 2306 (1964).

35. F. L. Mohler, Bur. Standards J. Res. 17, 849 (1936).

36. L. S. Frost, J. Appl. Phys. 32, 2029 (1961).

37. In reference 2, Boeckner and Mohler measured the variation of electron density across the tube and found that the average electron density was 0.7 times the value at the axis at the pressures of their experiments. Since the electron density correction discussed above should have no significant effect on the variation of electron density across the tube, no correction has been applied to the 0.7 factor.

FIGURE CAPTIONS

Fig. 1 Schematic diagram of drift tube and associated circuitry. A voltage square wave is applied to the electrode on the left and a dc ammeter measures the average current to the electrode on the right.

Fig. 2 Sample curve of average anode current versus twice the square wave frequency. The rounding off of the curve in the region around the breaking point is caused by diffusion. The data shown were obtained with $N_{Ar} = 1.21 \times 10^{19}$ cm^{-3} and $N_{Cs}/N_{Ar} < 10^{-7}$.

Fig. 3 Sample curve of drift time vs. drift distance for given value of E/N and N_{Cs}/N_{Ar}. The drift velocity is obtained from the slope of such curves. The data shown were obtained with $N_{Ar} = 1.31 \times 10^{19}$ cm^{-3} and $N_{Cs}/N_{Ar} < 10^{-7}$.

Fig. 4 Schematic diagram of apparatus.

Fig. 5 Electron drift velocity in cesium-argon mixtures. The square points were obtained for a cesium to argon density ratio of 10^{-7} or less. The lower solid curve represents the experimental results of Pack and Phelps for electron drift velocity in pure argon. The circular points were obtained at a constant density ratio of 6.9×10^{-6}. The three upper solid curves are the drift velocities calculated on the basis of three different assumed shapes for the cesium excitation cross section. The symbols "linear," "optical," and "classical" are explained in the text.

Fig. 6 The cross sections used to calculate the three upper solid curves in Fig. 5. These represent the magnitudes required for each shape, to give the best fit to experiment. The symbols "linear," "optical," and "classical" are explained in the text.

Fig. 7 Comparison of measured drift velocity with that calculated on the basis of a two threshold, linear cross section. The fit is slightly better around $E/N = 10^{-18}$ V-cm^2 than that obtained for a single threshold cross section.

Fig. 8 Comparison of theoretical and experimental cesium excitation cross sections. The dashed curves are theoretical calculations by Hansen (reference 32), Witting (reference 38), and Vainshtein, et al (reference 34). The solid curves are two different representations of the present experimental results, as explained in the text.

Fig. 9 Comparison of experimental measurements of the momentum transfer cross section in cesium. The curve labeled Boeckner and Mohler (revised) is based on the data of reference 2, as explained in the appendix. The other curves shown are from Brode (reference 1), Mullaney and Dibelius (reference 4), Chen and Raether (reference 5), Morgulis and Korchevoi (reference 6), Harris (reference 7), Roehling (reference 8) and Meyerand and Flavin (reference 9).

Dwg. 745A937

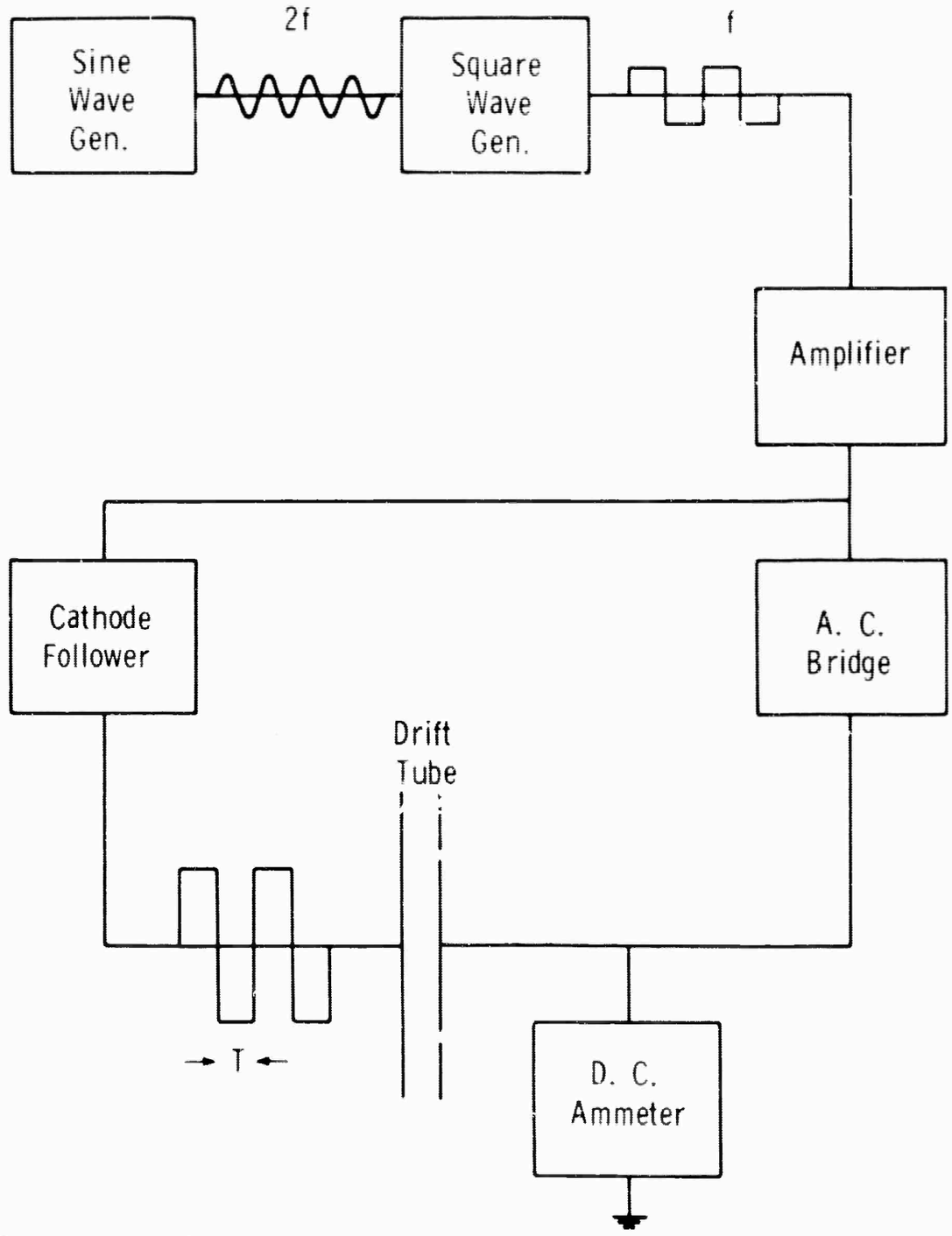

Fig. 1—Schematic diagram of drift tube and associated circuitry. A voltage square wave is applied to the electrode on the left and a dc ammeter measures the average current to the electrode on the right.

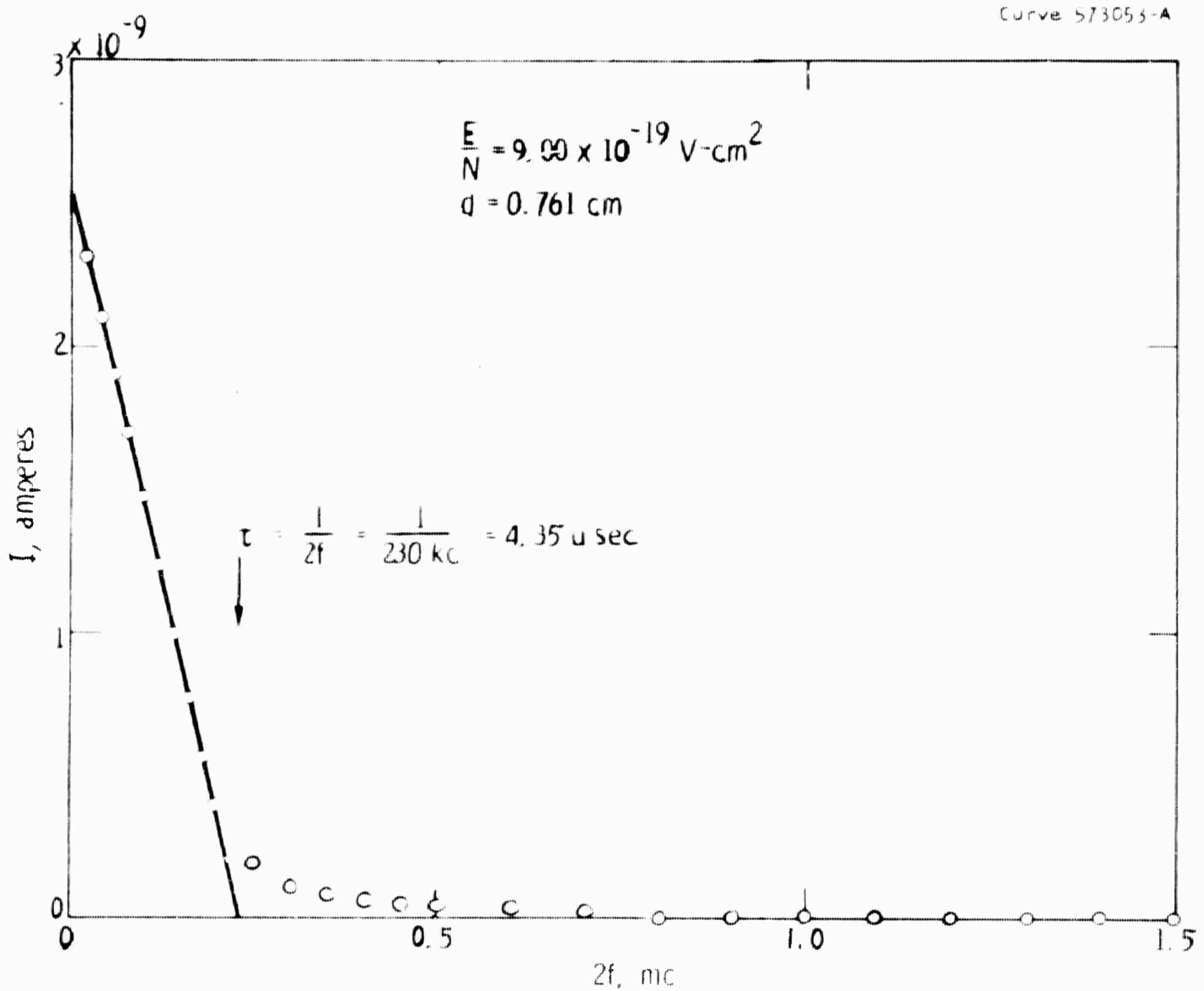

Fig. 2—Sample curve of average anode current vs. twice the square wave frequency. The rounding off of the curve in the region around the breaking point is caused by diffusion. The data shown were obtained with $N_{Ar} = 1.31 \times 10^{-19}$ cm^{-3} and $N_{Cs}/N_{Ar} < 10^{-7}$.

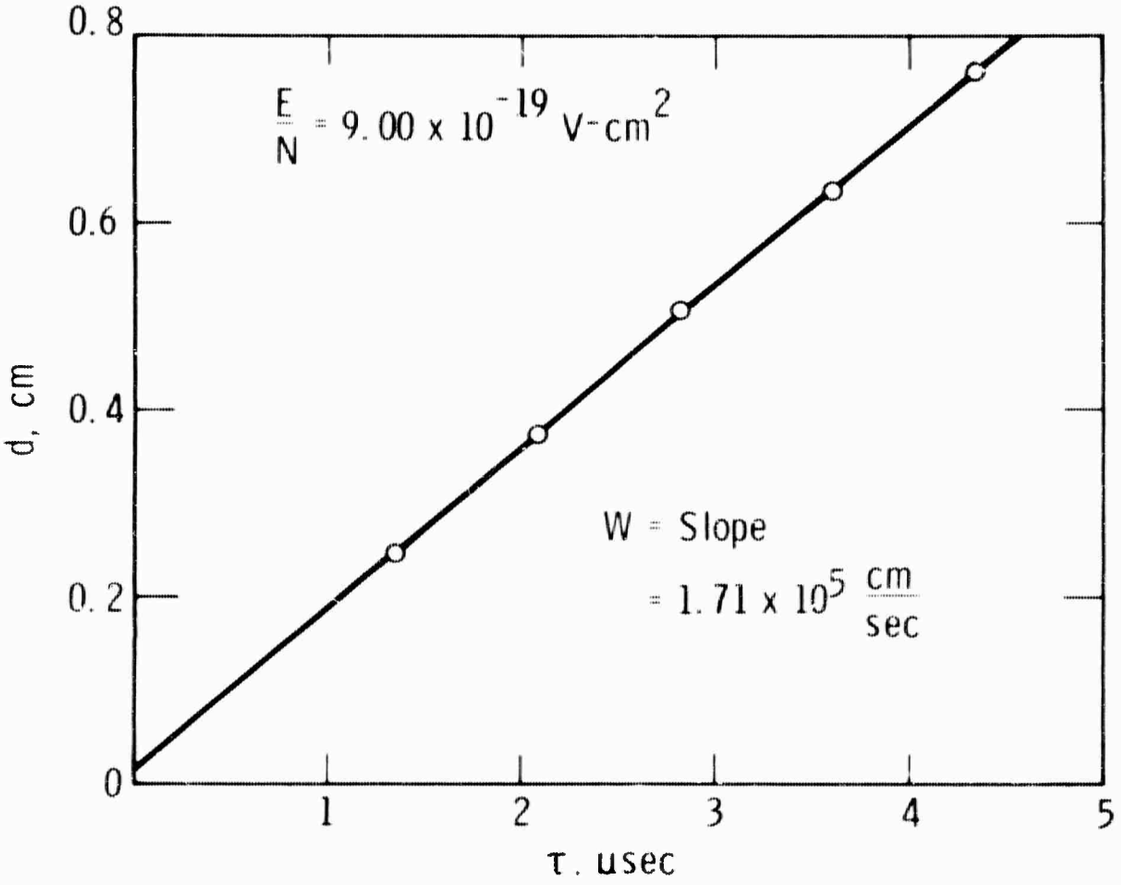

Fig. 3—Sample curve of drift time vs. drift distance for given value of E/N and N_{Cs}/N_{Ar}. The drift velocity is obtained from the slope of such curves. The data shown were obtained with

$$N_{Ar} = 1.31 \times 10^{-19}\ cm^{-3} \text{ and } N_{Cs}/N_{Ar} < 10^{-7}$$

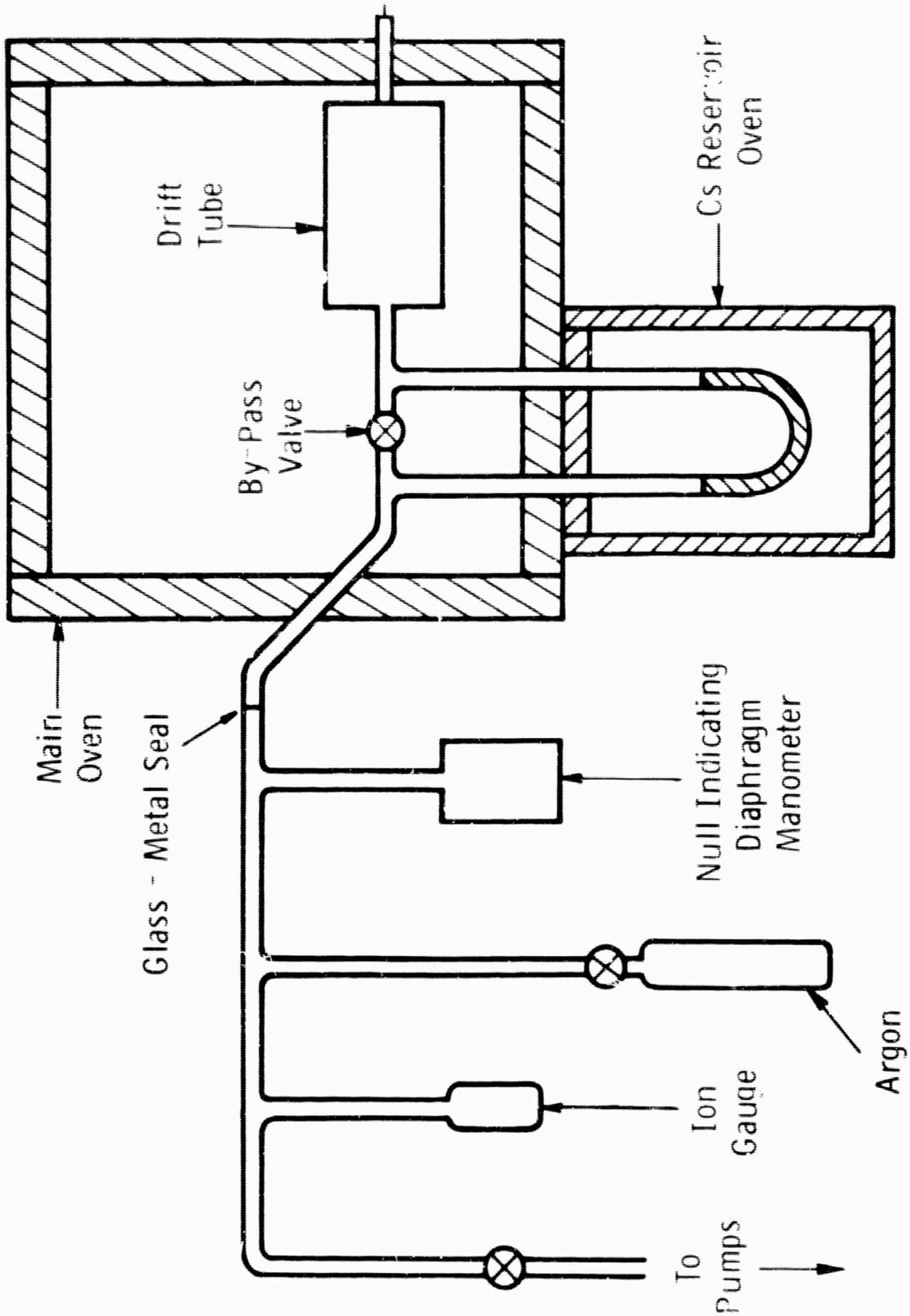

Fig. 4—Schematic diagram of apparatus

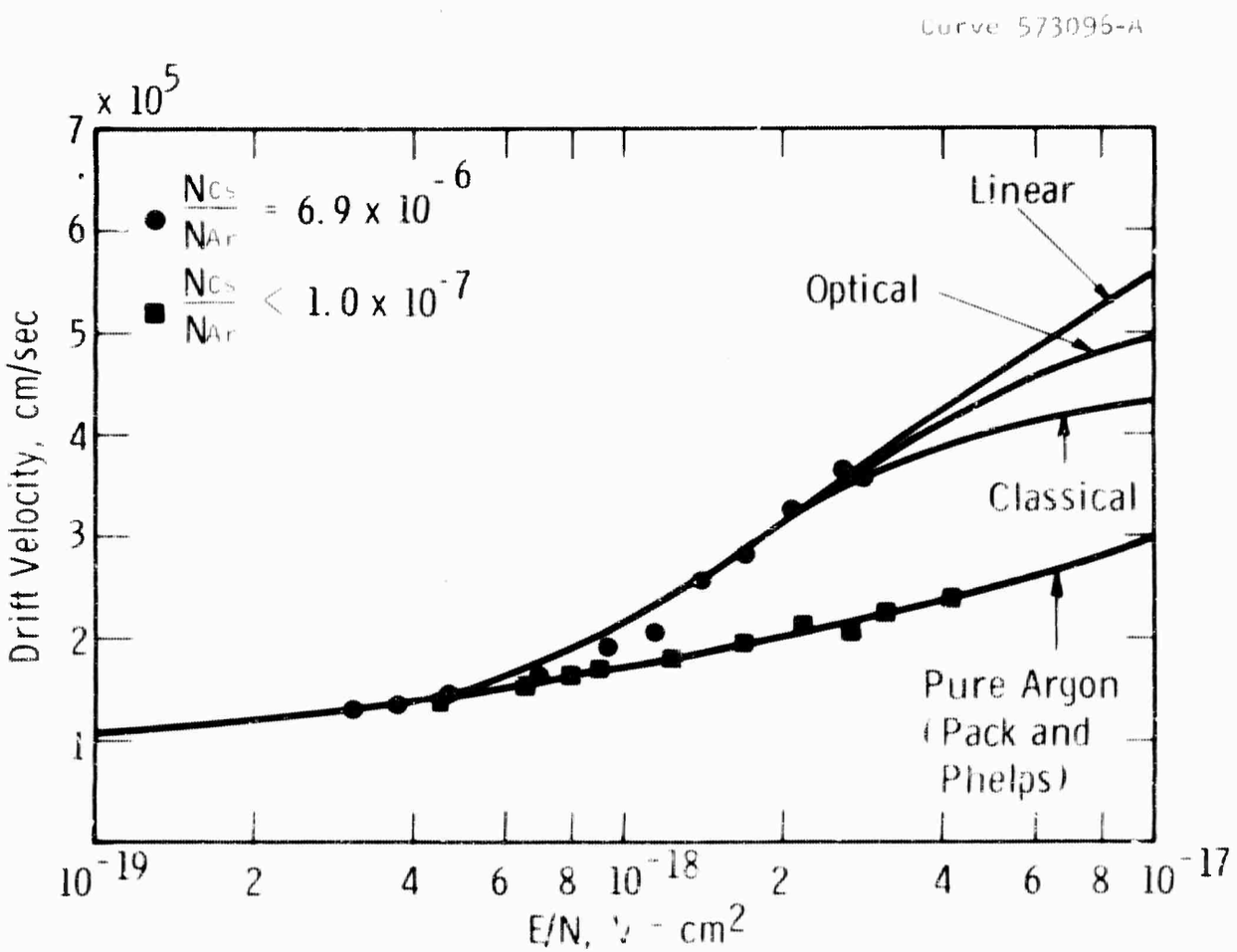

Fig. 5—Electron drift velocity in cesium-argon mixtures. The square points were obtained for a cesium to argon density ratio of 10^{-7} or less. The lower solid curve represents the experimental results of Pack and Phelps for electron drift velocity in pure argon. The circular points were obtained at a constant density ratio of 6.9×10^{-6}. The three upper solid curves are the drift velocities calculated on the basis of three different assumed shapes for the cesium excitation cross section. The symbols "linear," "optical," and "classical" are explained in the text.

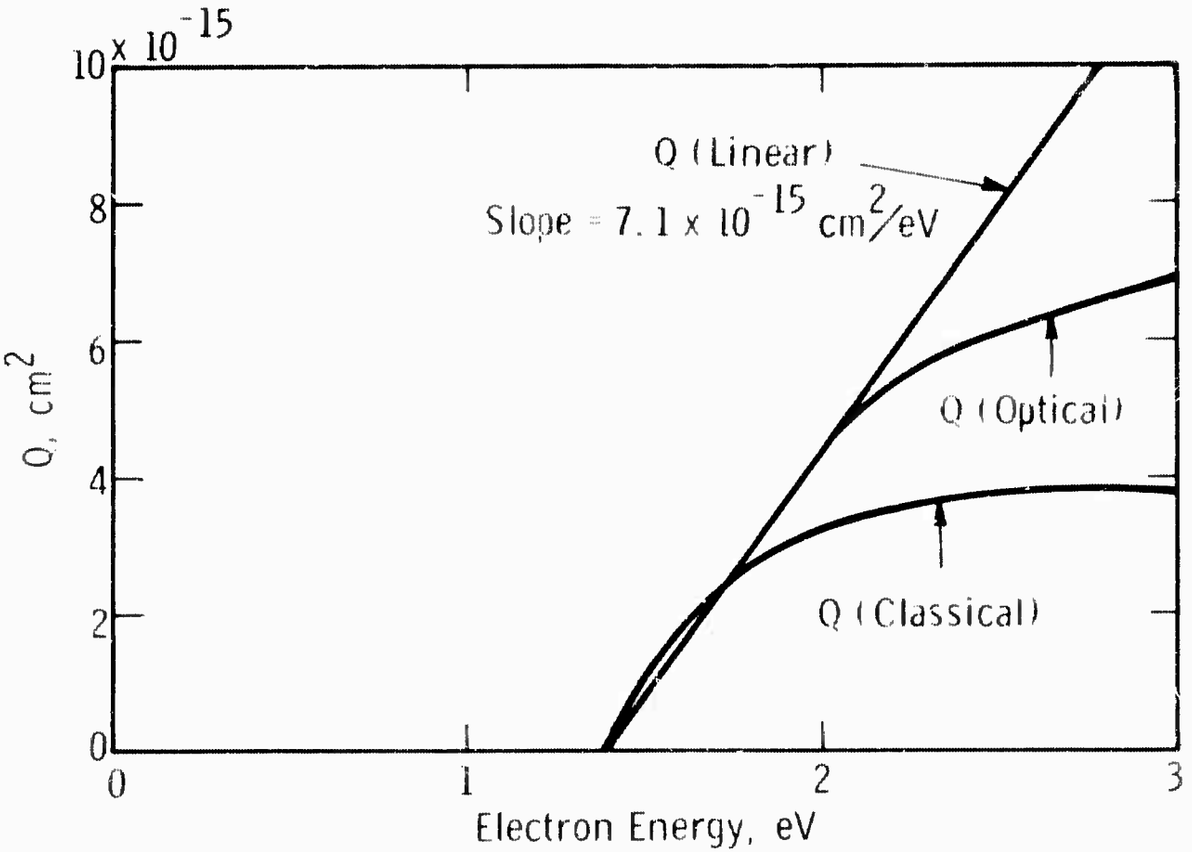

Fig. 6—The cross sections used to calculate the three upper solid curves in Fig. 5. These represent the magnitudes required for each shape, to give the best fit to experiment. The symbols "linear," "optical," and "classical" are explained in the text.

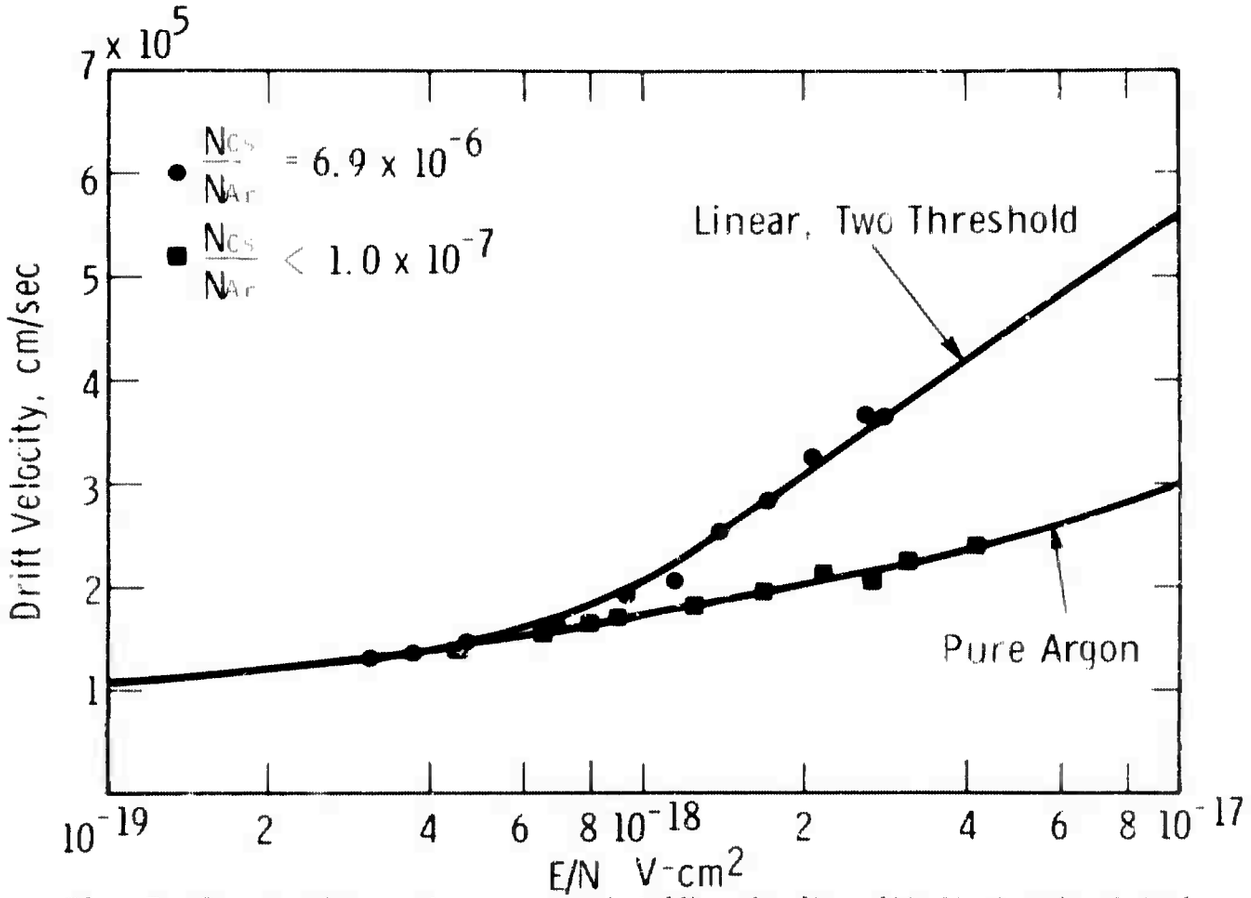

Fig. 7—Comparison of measured drift velocity with that calculated on the basis of a two threshold, linear cross section. The fit is slightly better around E/N = 10^{-18} V-cm^2 than that obtained for a single threshold cross section

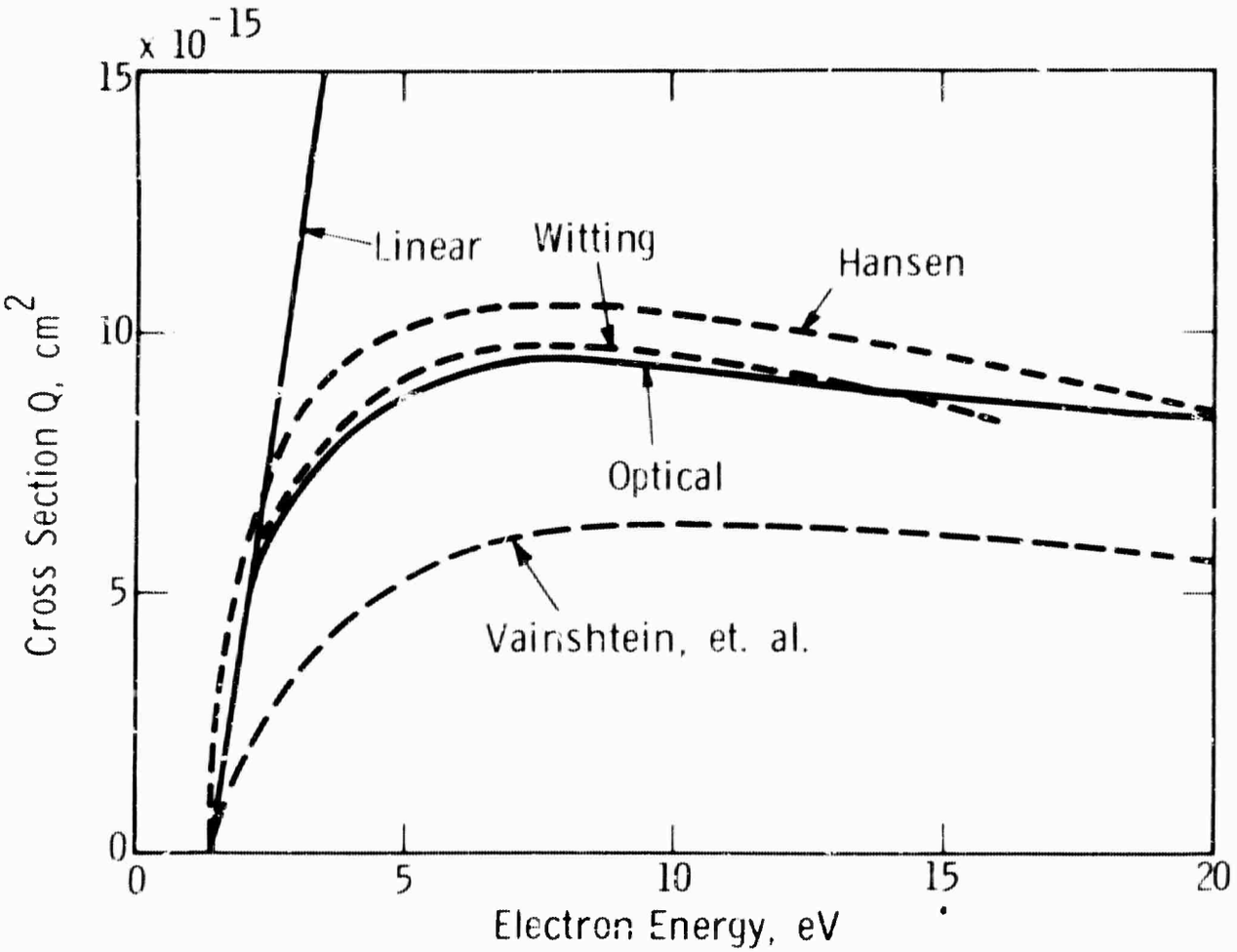

Fig. 8—Comparison of theoretical and experimental cesium excitation cross sections. The dashed curves are theoretical calculations by Hansen (reference 32), Witting (reference 38), and Vainshtein et al (reference 34). The solid curves are two different representations of the present experimental results, as explained in the text.

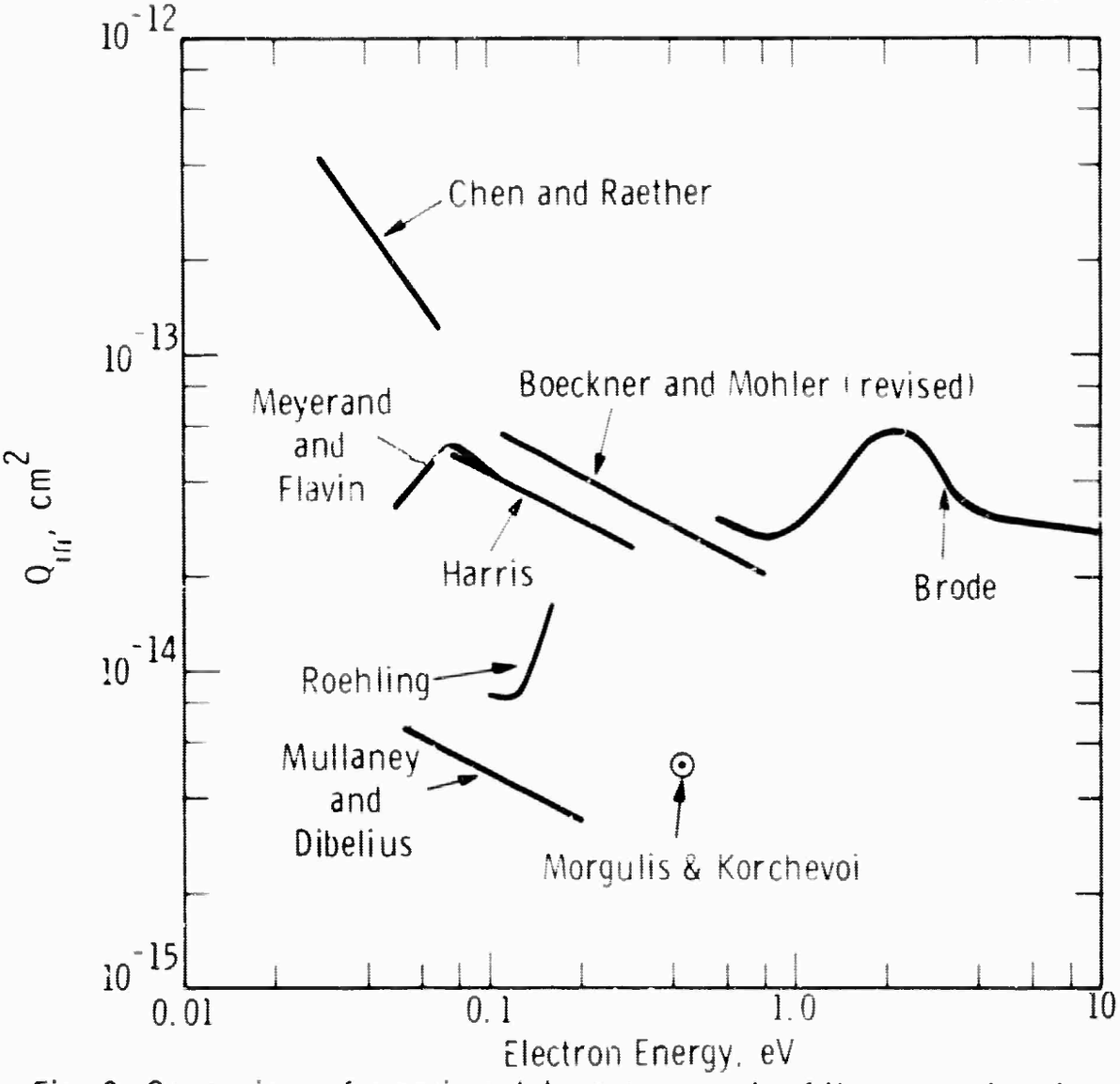

Fig. 9—Comparison of experimental measurements of the momentum transfer cross section in cesium. The curve labeled Boeckner and Mohler (revised) is based on the data of reference 2, as explained in the appendix. The other curves shown are from Brode (reference 1), Mullaney and Dibelius (reference 4), Chen and Raether (reference 5), Morgulis and Korchevoi (reference 6), Harris (reference 7), Roehling (reference 8) and Meyerand and Flavin (reference 9)

Table 1 Cross Sections Derived from Boeckner & Mohler

1	2	3	4	5
Electron Energy	Q_m	ν/N (uncorrected)	ν/N (corrected for electron density)	ν/N (corrected for Cs pressure)
0.222 eV	1.4 x 10^{-14} cm^2	0.592 x 10^{-6} cm^3/sec	1.61 x 10^{-6} cm^3/sec	1.22 x 10^{-7} cm^3/sec
.235	2.(	.872	1.61	1.18
.263	2.4	1.10	1.51	1.07
.282	3.1	1.58	1.58	1.08
.333	3.3	1.70	1.70	1.13
.400	2.9	1.65	1.65	1.04

Appendix II Drift Velocity in Cesium-Argon Mixtures

$N_{Cs}/N_{Ar} < 1.0 \times 10^{-7}$		$N_{Cs}/N_{Ar} = 6.9 \times 10^{-6}$	
E/N (V-cm^2)	W (cm/sec)	E/N (V-cm^2)	W (cm/sec)
4.51×10^{-19}	1.39×10^{5}	3.04×10^{-19}	1.32×10^{5}
6.53×10^{-19}	1.54×10^{5}	3.73×10^{-19}	1.33×10^{5}
7.93×10^{-19}	1.66×10^{5}	4.67×10^{-19}	1.44×10^{5}
9.00×10^{-19}	1.71×10^{5}	6.91×10^{-19}	1.61×10^{5}
1.24×10^{-18}	1.80×10^{5}	9.33×10^{-19}	1.90×10^{5}
1.69×10^{-18}	1.96×10^{5}	1.15×10^{-18}	2.04×10^{5}
2.18×10^{-18}	2.12×10^{5}	1.40×10^{-18}	2.50×10^{5}
2.70×10^{-18}	2.06×10^{5}	1.71×10^{-18}	2.81×10^{5}
3.11×10^{-18}	2.26×10^{5}	2.07×10^{-18}	3.25×10^{5}
4.17×10^{-18}	2.40×10^{5}	2.59×10^{-18}	3.67×10^{5}
		2.85×10^{-18}	3.53×10^{5}